EPJ manuscript No.
(will be inserted by the editor)

Collective excitations involving spin and isospin degrees of freedom

Hiroyuki Sagawa[1], Gianluca Colò[2], Xavier Roca-Maza[2], and Yifei Niu[3]

[1] RIKEN Nishina Center, Wako 351-0198, Japan and Center for Mathematics and Physics, University of Aizu, Aizu-Wakamatsu, Fukushima 965-8560, Japan
[2] Dipartimento di Fisica, Università degli Studi di Milano and INFN, Sezione di Milano, 20133 Milano, Italy
[3] School of Nuclear Science and Technology, Lanzhou University, Lanzhou 730000, China

Received: date / Revised version: date

Abstract. In this paper, we discuss some new important developments in the study of isobaric analog states (IAS) and Gamow-Teller resonances (GTR). In the case of the IAS, we have shown the importance of taking into account charge symmetry breaking (CSB) and charge independence breaking (CIB) forces, in order to reconcile the reproduction of the IAS energy in ^{208}Pb with the reproduction of some very basic observable like the neutron skin which, in turn, is strongly correlated with the density dependence of the symmetry energy. Isospin symmetry breaking terms can increase the energy of the IAS associated with Skyrme EDFs that produce a reasonable value of the neutron skin. In particular, this has been shown in the case of the SAMi functional. The GTR has a large damping width and its strength is experimentally found to be quenched with respect to standard RPA calculations. We have revised the PVC model for the width of giant resonances using the Skyrme force consistently for RPA (QRPA) and (quasi-)particle-vibration couplings (PVC or QPVC) calculations. We apply this model to the study of the GTR both in magic and open-shell nuclei. The results are in very good agreement with the experimental findings. The remaining discrepancies point to the necessity of fine tuning of the spin, spin-isospin, and spin-orbit terms in the existing EDFs. Some detailed formulas of CSB and CIB energy densities are given in the Appendix.

PACS. 2 1.10.Hw, – 2 1.10.Re, – 2 1.30.x, – 2 1.60.n

1 Introduction

The spin-isospin response and the spin-isospin terms of the effective nucleon-nucleon interaction are fundamentally important subjects in nuclear physics and astrophysics. The Gamow-Teller (GT) giant resonances have been known for many years [1–4] as the charge-exchange spin-excitations which can be classified as "allowed" transitions in analogy with the nuclear β-decay: they involve the transfer of one unit of total angular momentum as induced by the operator

$$\hat{O}_{\rm GT} = \sum_{i=1}^{A} \boldsymbol{\sigma}_i t_{\pm}(i). \tag{1}$$

The magnetic dipole (M1) transitions are observed in the non charge-exchange channel, and involve both the spin and the orbital angular momentum operators [1,3]. In the electromagnetic case, the operator reads

$$\hat{O}_{\rm M1} = \sum_{i=1}^{A} \left[g_s(i)\boldsymbol{\sigma}_i + g_l(i)\boldsymbol{\ell}_i \right], \tag{2}$$

where g_s has the values 5.586 and -3.826 for protons and neutrons, respectively, in units of the nuclear magneton $\mu_N = \frac{e\hbar}{2mc}$; in the same units, g_l has the values 1.0 and 0.0, respectively. In the case of the interaction with strong probes, one should expect different weights as we will hint below.

It has been argued that these spin-isospin operators (1) and (2) need to be quenched in order to reproduce the experimental values of the transition strengths [5,6]. In fact, experimental GT and M1 strength distributions show a substantial quenching compared to the relevant theoretical predictions by the shell model (SM) and the Random Phase Approximations [7–12]. There is a substantial difference between the two cases. While in the GT case a model-independent sum rule characterizes the difference between the total strengths S in the t_- and t_+ channels, namely

$$S_- - S_+ = 3(N - Z), \tag{3}$$

and one can define the quenching with respect to it, this is not the case for the M1 operator. In this latter case one can discuss the quenching with respect to theoretical calculations only. A similar quenching effect also occurs in the observed magnetic moments of almost all nuclei, when

Send offprint requests to:

compared to the single-particle unit (i.e., to the Schmidt value) [1,5,6].

The quenching effect of the spin-isospin response impacts on many physical and astrophysical processes such as the neutrino-less double-β ($0\nu\beta\beta$) decay [13], the spin susceptibility of asymmetric nuclear matter [14], the neutrino-nucleus reaction cross sections [15], the mean free path of neutrinos in dense neutron matter [16,17], the dynamics of core-collapse supernova and the nucleosynthesis process [18], the cooling of O-Ne-Mg cores in stars with mass around 8-10 $M_\odot$ [19–21] as well as the cooling of proto-neutron stars [22], and the spin-response to strong magnetic fields in magnetars [23].

Magnetic moments are the subject of extensive compilations, and GT strengths have been measured in a number of cases by means of charge-exchange reactions like (p,n) or (^{3}He, t). The quenching of magnetic moments and GT strengths has been extensively studied by taking into account the mixing of 1 particle-1 hole (1p-1h) configurations with 2 particle-2 hole (2p-2h) or higher configurations, the meson exchange currents, and the coupling to the Δ-baryon, which has $J^\pi = 3/2^+$ and $T = 3/2$ so that it can be regarded as a 1^+ nucleon resonance in which the quarks rearrange their quantum numbers [5,6,24–26]. Concerning the quenching of the GT Ikeda sum rule (3) [7], there have been many strong discussions whether the effect of many particle-many hole states or the coupling to the Δ-resonance had to be considered to be the dominant contribution [25,26]. After a long debate [28], experimental investigations by means of charge-exchange (p,n) and (n,p) reactions on ^{90}Zr have revealed that about 90% of the GT total strength is found in the energy region up to $E_{\rm x}$=50 MeV [9,4]. This demonstrates the importance, for the quenching problem, of the coupling between the GT resonance and many particle-many hole configurations (mostly, 2p-2h coupling produced by both the central and tensor forces [24]), although the coupling to the Δ-isobar is not completely excluded. **It should be also noticed that the GT strength can couple with spin-quadrupole excitations with $J^\pi = 1^+$, mainly by tensor interactions. In ref. [27], it was shown that about 10% of the GT sum rule strength is shifted to higher excitation energy region $Ex > 30MeV$.**

Starting from Eq. (2), one can define isoscalar (IS) and isovector (IV) M1 transitions. The angular part is relevant only for deformed nuclei. Thus, if we restrict ourselves to the spin part, the IS and IV operators read

$$\hat{O}_{\rm M1,IS} = \sum_{i=1}^{A} g_s(i)\boldsymbol{\sigma}_i, \tag{4}$$

$$\hat{O}_{\rm M1,IV} = \sum_{i=1}^{A} g_s(i)\boldsymbol{\sigma}_i t_z(i). \tag{5}$$

The isovector (IV) M1 transitions can be, and have been, measured by using γ-ray and electron scattering experiments. On the other hand, the empirical information concerning isoscalar (IS) M1 transitions is very scarce. This is due to the fact that the IS spin g-factor is much smaller than the IV one, i.e., $(g_s^{IS}/g_s^{IV})^2 \approx 1/30$, as one can deduce from the values mentioned below Eq. (2), for the electromagnetic processes. For the hadronic processes, the IS spin coupling is also much smaller than the IV one, namely $V_\sigma^{IS}/V_\sigma^{IV} < 1/6$ at intermediate reaction energy [29].

One clear observation of IS spin excitation is the 1^+ state at 12.71 MeV in ^{12}C seen by electron scattering. In this case, no quenching in the IS M1 strength is observed, as compared with SM calculations; rather, the measurement indicates a large enhancement of the GT strength as compared with the SM. Recently, both IS and IV spin M1 transitions, have been investigated by high-resolution proton inelastic scattering measurements at $E_{\rm p}$ = 295 MeV [30]. The IV spin M1 transitions induced by the operator (5) can be regarded as analogous to the GT transitions, while the IS spin M1 transitions induced by the operator (4) are free from the coupling to the Δ-isobar because of isospin selection rules. In other words, the quenching of IS strength should be only due to the couplings to higher-order p-h configurations such as as 2p-2h, 3p-3h and so on. In this respect, the measurement of IS spin excitations may provide an important information on the quenching mechanism of spin-dependent excitations in nuclei.

The IS spin-triplet pairing correlations have been reported to play an important role in enhancing the GT strength near the ground states of nuclei with N≈Z [31–34]. At the same time, the accumulated sum rule of the GT strength in the shell model calculations is quenched by ground state correlations due to the IS pairing [35]. The IS paring is also found to be important to reduce the $0\nu\beta\beta$ decay matrix elements [36].

As the last but not least interesting topic related to spin-isospin excitations, we should mention that double charge-exchange (DCX) states induced by heavy-ion beams at intermediate energies [37,38] attract currently a lot of interest, in connection with new collective excitations such as double isobaric analog states (DIAS) and double Gamow-Teller giant resonances (DGTR). In the 1980s, DCX reactions were performed by using pion beams, i.e. (π^+,π^-) and (π^-,π^+) reactions have been studied. Through these experimental studies, the double isobaric analog states (DIAS), the dipole giant resonance (GDR) built on the IAS and the double dipole resonance states (DGDR) were identified [39–41]. However, the DGTRs were not found in the pion double charge-exchange spectra. In the middle of the 1990s, experiments were performed at energies of 76 and 100 MeV/A with the hope that the DGTR might be observed in the ^{24}Mg(^{18}O, ^{18}Ne)^{24}Ne reaction [42]. However, no clear evidence of DGTR was found in this reaction either. This is mainly because the (^{18}O, ^{18}Ne) reaction is a (2n, 2p)-type reaction, and even the single GT t_+ resonance induced by the (n,p) reaction is weak in the N=Z nucleus ^{24}Mg. A new research program based on a new reaction, namely (^{12}C, ^{12}Be(0_2^+)), has been planned at the RIKEN RIBF facility with high intensity heavy-ion beams at the optimal energy of 250 MeV/A to excite the spin-isospin response [43]. A big advantage of this reac-

tion is based on the fact that it is a (2p,2n)-type DCX reaction, and one can use a neutron-rich target to excite the DGT strength. Although many theoretical efforts have been paid for studies of double-β decays, DGT strengths corresponding to the double-β decays are still too small to be identified in these experiments. Recently, shell-model calculations were performed to study the DGTR of ^{48}Ti [44]. On the other hand, the DGT strength distributions have been studied by using the sum rule approach [45–48] to establish a possible unit cross section of DGTR in comparison with the strength of DIAS.

In summary, many different topics are experiencing a significant progress currently. In the spirit of this Topical Issue, we have picked up two specific subjects that we shall discuss, namely the study of the single IAS including the contribution of charge-symmetry breaking (CSB) and charge-independence breaking (CIB) interactions and the study of GTR within the framework of the particle-vibration coupling model. In the past, P.F. Bortignon devoted his interest to both these topics (cf. Refs. [49–51]), and we are glad to contribute to his memory with recent developments in the same topics.

2 IAS and CSB and CIB interactions

The IAS is one of the well established properties of nuclei that is measured accurately, and is essentially sensitive to the isospin symmetry breaking (ISB) in the nuclear medium. The main ISB part of the nuclear Hamiltonian is the Coulomb interaction.

Exactly because the IAS energy is such a precisely measured quantity, if there is an inconsistency between this quantity and the knowledge of other nuclear properties, this is a serious issue. In this Section, we discuss the case of the nuclear symmetry energy. In nuclear physics it is customary to give the name of Equation of State (EoS) to the function energy per particle, E/A, in uniform matter; the reason is clearly that from this function one can extract directly the pressure as a function of the density. Nuclear matter is characterized by a total density ρ and a neutron-proton asymmetry β defined as $\beta \equiv (\rho_n - \rho_p)/\rho$; thus, the EoS is the function $E/A(\rho, \beta)$. It is customary in the literature to assume isospin symmetry because Coulomb forces are taken out in infinite matter. In this conditions, such function can be expanded in even powers of β, and by stopping at second order one can write

$$\frac{E}{A}(\rho, \beta) = \frac{E}{A}(\rho, \beta = 0) + S(\rho)\beta^2. \qquad (6)$$

This equation defines the so-called symmetry energy $S(\rho)$, that is, the difference between the energy per particle E/A in neutron and symmetric matter. Knowledge of the symmetry energy is mandatory in order to understand neutron-rich matter and also the physics of neutron stars.

The parameters that encode our current understanding of the symmetry energy are denoted by J, L and $K_{\rm sym}$. J is the value of the symmetry energy at the saturation density of symmetric matter, $\rho_0 \approx 0.16$ fm^{-3}. Its value is deemed to be between 28.5 MeV and 34.5 MeV [52]. The density dependence of the symmetry energy around ρ_0 is reflected by the first and second derivative. The so-called "slope parameter" L is defined as $3\rho_0\ S'(\rho_0)$, while $K_{\rm sym} \equiv 9\rho_0^2\ S''(\rho_0)$. $K_{\rm sym}$ is basically unknown, and the error on L is significantly larger than the error on J: ranges between $\approx$ 40-75 MeV or between $\approx$ 30-90 MeV are mentioned in Refs. [53–55, 52]. A strong correlation between L and the neutron skin $\Delta R_{\rm np} \equiv \langle r_n^2\rangle^{1/2} - \langle r_p^2\rangle^{1/2}$ of a heavy nucleus like ^{208}Pb has been pointed out by many authors, starting from the seminal work of Ref. [56]. This correlation is also quite understandable: the larger is the change in symmetry energy as a function of the density, the more convenient the system finds it to push the excess neutrons to a lower density region, that is, towards the surface.

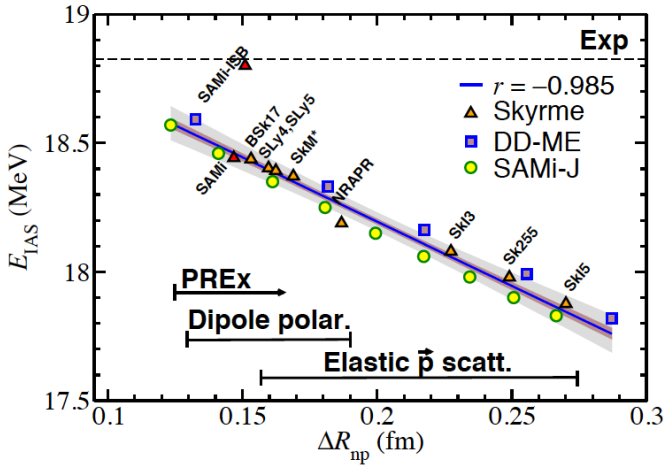

Fig. 1. Energy of the IAS as a function of ΔR_{np} with various EDFs. The dashed line marks the experimental value for E_{IAS}. The lines in the lower part of the figure indicate the experimental results associated with the neutron skin. They are obtained, respectively, from the polarized electron parity violation experiment PREx, from the measurement of giant dipole resonances, and from the analysis of polarized proton scattering.

We cannot accept that the values of the neutron skin (and, as just mentioned, of L) do not match with the measured values of the energy of the IAS, $E_{\rm IAS}$. In Fig. 1 we show that calculations of $E_{\rm IAS}$ performed with many state-of-the-art nuclear Energy Density Functionals (EDFs) are well correlated with the neutron skin. Yet, if we extrapolate, an hypothetical EDF that could match the experimental finding for $E_{\rm IAS}$ would not be consistent with the available measurements of the neutron skin, that is also displayed in the figure by means of horizontal lines.

To be more specific about the models whose results are shown in Fig. 1, let us discuss the two families SAMi-J and DD-ME. In the former case, starting from the prototype SAMi functional [57] a systematically varied family has been generated, by keeping a similar quality of the original fit and varying the values of J and L. In addition, a family

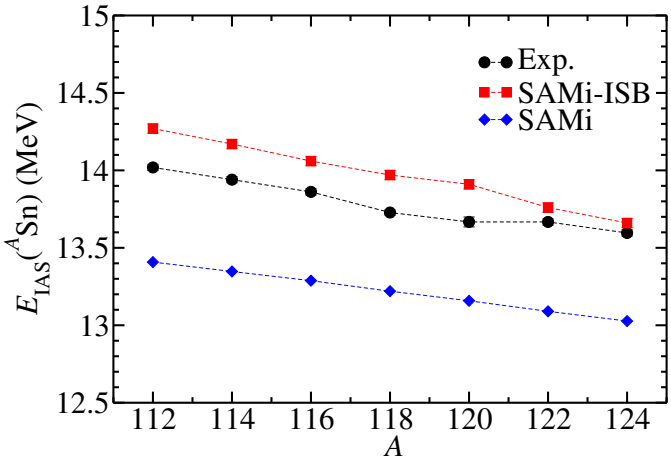

Fig. 2. Energies of IAS in Sn isotopes. Experimental data are shown by black dots, while calculated results of SAMi and SAMi+ISB are shown by blue diamonds and red squares, respectively.

based on the systematic variation of J and L with respect to a relativistic mean field (RMF) model with density dependent meson-nucleon vertices (DD-ME), is also introduced. These functionals provide values of the neutron skin through the Hartree-Fock (HF) or Hartree solution for the ground-state; and they provide, self-consistently, the IAS energy via the charge-exchange Random Phase Approximation (RPA). Results associated with other Skyrme interactions are also plotted. We found a serious discrepancy, around 0.5–1 MeV, between the calculated and experimental values of $E_{\rm IAS}$, for all the EDFs in Fig. 1.

To solve this puzzle, we have reconsidered all possible contributions to the IAS energy that have not been considered with sufficient care in self-consistent calculations so far. Then, we propose a new parametrization SAMi-ISB for Skyrme-like EDF that reconciles standard nuclear properties (saturation density, binding energy and charge radii of finite nuclei) with both our current understanding of the density behaviour of the symmetry energy and the reproduction of the IAS energy of ^{208}Pb.

We have self-consistently included for the first time within the HF+RPA framework all known contributions that break the isospin symmetry [58]. All of these contributions have been calculated in a model-independent way except for ISB terms originated from the strong nuclear force (cf. also [59]). We have fixed only two free parameters in the CSB and CIB terms, and we have shown that this allows for a good reproduction of the IAS energy of ^{208}Pb without compromising the other properties of nuclear matter and finite nuclei. This new Skyrme set is named SAMi-ISB. The calculated results give a fine agreement with the experimental excitation energy of IAS in ^{208}Pb reconciling realistic symmetry energy parameters and the neutron skin as is shown in Fig. 1. The energies of IAS in Sn isotopes are also improved by SAMi-ISB as is shown in Fig. 2.

In the Appendix, we provide the full details related to our choice of CSB-CIB interactions. Those interactions are based on previous studies of ISB effects in the nuclear medium [60,61]. In particular, we derive the full mean-field associated with such interactions, that enters the HF equations. It should be noted that at this level of approximation (HF), contrary to other proposed effective interactions [62] and in agreement with Brueckner-Hartree-Fock calculations of Ref. [63], they also provide contributions to symmetric nuclear matter. In Fig. 3, we show different theoretical predictions for ISB effects on the symmetric matter equation of state ΔE_{ISB} (left panel) and CSB effects on the single-particle potential $U_{CSB} = U_p - U_n$ (right panel), both as a function of the Fermi momentum. Specifically, Brueckner-Hartree Fock (BHF) calculations of Ref. [63] (black circles) are displayed together with predictions by SAMi-ISB [58] (blue dashed line). In addition, in the left panel of Fig. 3, a grey band is displayed based on the investigations of Ref. [62] where different Skyrme interactions have been modified for the study of nuclear masses with $N \approx Z$. Specifically, ISB terms are added to the Skyrme functional and fitted to experimental mirror and triplet displacement energies of isospin multiplets. Despite some difference in the CIB term with respect to the SAMi-ISB counterpart, the CSB effective interaction proposed in [62] is identical to the one employed in SAMi-ISB (as described in detail in the appendix). On the one side, the interaction proposed in Ref. [62] does not contribute to the energy per particle of symmetric nuclear matter (left panel of Fig. 3) while BHF calculations predict a non-zero contribution. SAMi-ISB has been fitted to the latter calculations, so the agreement is perfect. On the other side, the interaction in Ref. [62], solved within the HF approximation does contribute to the CSB single-particle potential. These results are plotted as a grey band in the right panel of Fig. 3. Specifically, the band has been obtained by considering the largest spread found in Ref. [62] (cf. Table 1 of this reference). The disagreement in the description of U_{CSB} is specially clear in the case of BHF calculations and SAMi-ISB while the results of Ref.[62] lie between them. The discrepancy between BHF and SAMi-ISB results for U_{CSB} are due to the following. As mentioned, in SAMi-ISB ΔE_{ISB} from the same BHF calculations have been explicitly included in the fit. ΔE_{ISB} depends only on the CIB interaction proposed in the SAMi-ISB functional since CSB does not contribute to symmetric nuclear matter (cf. Appendix). If CSB effects are neglected the description of SAMi-ISB to E_{IAS} in ^{208}Pb would be worse than that of SAMi, meaning that CIB interactions consistent with the BHF calculations of Ref. [63] will not help in the description of the IAS, but quite the contrary. Therefore, in order to reproduce the experimental energy of the IAS in ^{208}Pb SAMi-ISB have a large contribution to the CSB channel, much larger than it would be expected from the corresponding scattering lengths in the vacuum [60–62]. These results, among others, point towards the fact that we need a deeper physical insight into ISB effects in the medium. On this regard, it is important to note, that in both Refs. [58,62], a simplified form of the ISB ef-

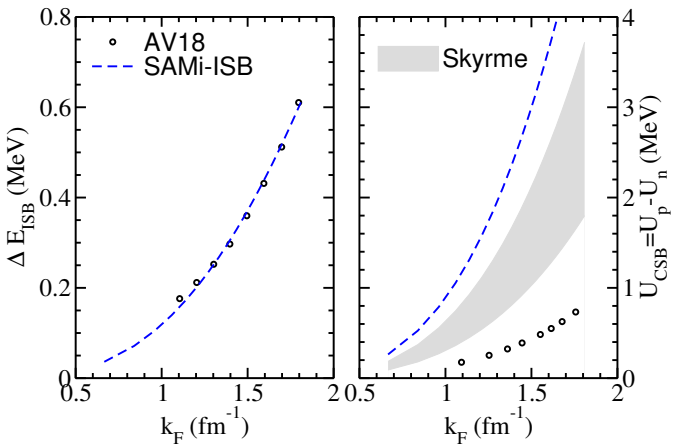

Fig. 3. Results from CSB and CIB interactions within a Brueckner Hartree-Fock calculations and from various Skyrme models. See the text for a full discussion.

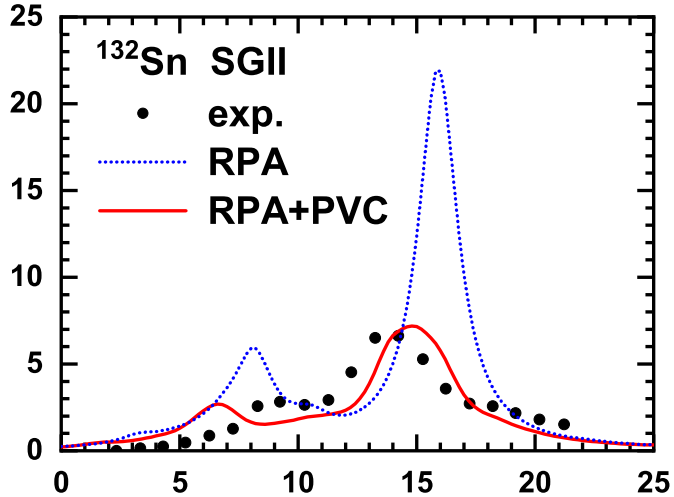

Fig. 4. The GT strength distributions of ^{132}Sn calculated by RPA and RPA+PVC model based on Skyrme interaction SGII, in comparison with experimental data extracted from the (p,n) reaction [64].

fective interactions were used. Further improvements are under development by these two groups in order to better understand ISB interactions in the medium.

3 GTR and PVC coupling

As discussed in the Introduction, the Gamow-Teller (GTR) is an important spin-isospin excitation. Most of the properties we have mentioned there are gross properties such as centroid excitation energy and total strength. We should add here that the GTRs have a conspicuous spreading width, and the coupling to low-lying surface vibrations is essential to reproduce this large width observed in the resonance region. Therefore, in order to describe the detailed distribution of the GT transition strength experimentally observed, one needs to go beyond RPA, and include more correlations such as coupling to phonons. Particle vibration coupling (PVC) is one of such approaches. Based on the Skyrme EDFs, a self-consistent RPA+PVC approach has been developed, where self-consistency means that the same Skyrme interaction is used in the calculation of Hartree-Fock (HF) ground state, residual interaction in RPA, as well as the vertex of PVC [51].

With the development of radioactive beam facilities (RIBFs), the measurement of GTRs can be extended to nuclei far from the stability line. Recently, using the inverse-kinematics charge-exchange (p,n) reaction with a radioactive isotope beam, the GTR of ^{132}Sn has been measured [64]. This provides a good opportunity to test the predictive power of our model in unstable nuclei.

Thus, in Fig. 4, the comparison between experimental data and theoretical results for the GT strength distribution is shown. The theoretical results are calculated by RPA and RPA+PVC models based on the Skyrme interaction SGII [65]. The smearing parameter $\Delta = 1$ MeV is used in the calculations, to simulate the experimental resolution. At the RPA level, there are two peaks. For the higher peak, the RPA calculation overestimates the centroid energy of the GTR, and cannot give a description of the full width, while for the lower one, the RPA gives a lower and stronger peak compared to the experimental bump at 9 MeV. The main components for the higher peak in the RPA calculation are $\nu h_{11/2} \to \pi h_{9/2}$ and $\nu g_{9/2} \to \pi g_{7/2}$, and that for the lower peak is $\nu d_{5/2} \to \pi d_{3/2}$. From RPA to RPA+PVC, the high resonance peak is shifted downwards by about 1 MeV, and gets a significant spreading width. As a result, one sees a similar profile as compared to experimental data in the GTR region. The lower peak gets more smoothed out: however, it still exists and its energy is still lower than the experimental bump. The GT energy is a result of a delicate interplay between single-particle spin-orbit splittings and residual interaction. So the accurate description of both is necessary to reproduce the correct GT strength; this is highly demanding for current EDFs and the figure shows the limits of our present capability.

Due to the success of RPA+PVC model, we have further extended this model to the quasiparticle case for the description of superfluid nuclei, namely we have proposed the quasiparticle RPA (QRPA) + quasiparticle vibration coupling (QPVC) model in Ref. [66]. We take the nucleus ^{120}Sn as a benchmark to test our model. In Fig. 5, the GT strength distributions and cumulative sums, calculated in ^{120}Sn by QRPA and QRPA+QPVC using the Skyrme interaction SGII, are shown and compared with experimental data extracted from the (p,n) reaction [67]. Here, in fact, the GT data are deduced from the (p,n) cross section in a rough way, by using the relation $\sigma(0^o) = \hat{\sigma} F(q,\omega) B(\mathrm{GT})$ with the approximation $F(q,\omega) = 1$. As a pairing interaction, the surface type δ-force is adopted. In panel (a) one can see that going from QRPA to QRPA+QPVC the two peaks in the high energy resonance region merge to form a broader peak with a large spreading width of about 4.5 MeV, which is in good agreement with experimental data. Although the

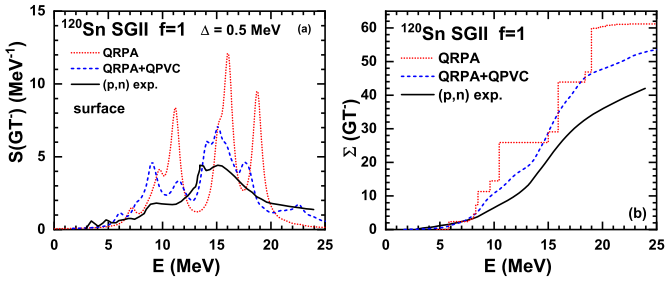

Fig. 5. The GT strength distributions [panel (a)] and cumulative sums [panel (b)] of ^{120}Sn calculated by QRPA and QRPA+QPVC model based on Skyrme interaction SGII, in comparison with experimental data extracted from (p,n) reaction [67]. The surface-type pairing interaction is adopted for the pairing channel of interaction. f is the ratio between the strength of isoscalar and isovector pairing.

low-energy peak becomes weaker from QRPA to QPVC, it appears to be still stronger than in the experimental data. In panel (b), the cumulative sum of GT strength is shown up to 25 MeV. At the QRPA level, the sum of GT$^-$ gives 103% of the Ikeda sum rule (considering the fact that the GT$^+$ strength is not removed from it), and at QRPA+QPVC level, the sum is quenched by about 15%. This means that with the inclusion of coupling with vibrational phonons, some strength is shifted to the higher energy region. However, the experimental data seem to point to a total strength which is about 20% lower than the QPVC result. Therefore, other effects like the coupling with high-energy, non-collective 2p-2h states, the inclusion of tensor force coupling, or the coupling with the Δ-isobar, together with the experimental uncertainty, should be responsible for the explanation of this difference.

4 Summary and future perspectives

The study of the nuclear excitations involving spin and isospin is not a new subject, but it is still very lively. This is also due to its relevance for applications in particle physics and astrophysics. In our Introduction, we have stressed how the properties of the GT and M1 excitations impact on a large host of phenomena taking place in nuclei that we study in terrestrial laboratories as well as in compact astrophysical objects like (proto-)neutron stars. At the same time, the development in experimental techniques has allowed to disentangle IS and IV M1 excitations, to access the quenching phenomena of the GTR with increasing accuracy, and to start observing double charge-exchange excitations. The experimental progress contributes to the liveliness of this field of research.

In this paper, we have focused on the IAS and GTR, by discussing some new important developments. In the case of the IAS, we have shown that, up to very recently, calculation based on EDFs have not been able to reconcile the reproduction of the IAS energy in ^{208}Pb with the reproduction of some very basic observable like the neutron skin which, in turn, is strongly correlated with the density dependence of the symmetry energy. In a recent work, some of us have been able to solve this puzzle by including all isospin symmetry breaking contributions in a consistent manner. Isospin symmetry breaking terms can increase the energy of the IAS associated with EDFs that produce a reasonable value of the neutron skin. In particular, this has been shown in the case of the SAMi functional.

While most of the isospin symmetry breaking terms are essentially model independent, this is not the case for the CSB-CIB terms of the effective nucleon-nucleon interaction. We have chosen a specific form and fit the parameters of these terms. More general understanding of this component of the effective force, in keeping also with the recent findings of other groups [62], should be envisaged.

The fact that isospin symmetry breaking in nuclei is anyway small, explains the fact that the IAS is a very narrow state. The GTR has a large damping width and its strength is experimentally found to be quenched with respect to standard RPA calculations. We have recently revised the PVC model for the width of giant resonances by dropping previously adopted approximations and using the Skyrme force consistently. We have applied this model to the study of the GTR both in magic and open-shell nuclei. The results are in very good agreement with the experimental findings. The remaining discrepancies point to the necessity of fine tuning of the spin, spin-isospin, and spin-orbit terms in the existing EDFs.

Appendix: CSB and CIB Skyrme-like interactions and associated HF potentials and energy density

A charge symmetry breaking potential can be generally defined as $V_{\rm CSB} = V_{nn} - V_{pp}$, while a charge independence breaking potential can be generally defined as $V_{\rm CIB} = \frac{1}{2}\left(V_{nn} + V_{pp}\right) - V_{pn}$. So an effective nucleon-nucleon potential can be build out of three parts: the charge independent part (isospin symmetry is fully preserved) plus the two previously defined breaking terms.

Following [60] [cf. Eqs. (18-21)] one can define Skyrme-like CSB and CIB potentials as follows,

$$V_{\rm CSB}(\boldsymbol{r}_1,\boldsymbol{r}_2) \equiv \frac{1}{4}\left[\tau_z(1)+\tau_z(2)\right]\Bigg\{ s_0(1+y_0P_\sigma) + \frac{1}{2}s_1(1+y_1P_\sigma)\left[\boldsymbol{D}'^2\delta(\boldsymbol{r}_1-\boldsymbol{r}_2)+\delta(\boldsymbol{r}_1-\boldsymbol{r}_2)\boldsymbol{D}^2\right] + s_2(1+y_2P_\sigma)\boldsymbol{D}'\cdot\delta(\boldsymbol{r}_1-\boldsymbol{r}_2)\boldsymbol{D}\Bigg\}, \quad (7)$$

and

$$V_{\rm CIB}(\boldsymbol{r}_1,\boldsymbol{r}_2) \equiv \frac{1}{2}\tau_z(1)\tau_z(2)\Bigg\{ u_0(1+z_0P_\sigma) + \frac{1}{2}u_1(1+z_1P_\sigma)\left[\boldsymbol{D}'^2\delta(\boldsymbol{r}_1-\boldsymbol{r}_2)+\delta(\boldsymbol{r}_1-\boldsymbol{r}_2)\boldsymbol{D}^2\right] + u_2(1+z_2P_\sigma)\boldsymbol{D}'\cdot\delta(\boldsymbol{r}_1-\boldsymbol{r}_2)\boldsymbol{D}\Bigg\}.$$

(8)

Here $\boldsymbol{D} \equiv \frac{1}{2i}(\boldsymbol{\nabla}_1 - \boldsymbol{\nabla}_2)$ acts on the right and $\boldsymbol{D}'$ is its complex conjugate acting on the left, while $P_{\tau/\sigma}$ are the usual projector operators in isospin and spin spaces, respectively. In Refs. [61,62], the isotensor-type CIB interaction was proposed. The Skyrme-type CIB can be written also in an isotensor form as

$$V^T_{\rm CIB}(\boldsymbol{r}_1,\boldsymbol{r}_2) \equiv \frac{1}{2}\left[3\tau_z(1)\tau_z(2) - \tau(1)\cdot\tau(2)\right]\Bigg\{u_0^T(1+z_0^T P_\sigma) + \frac{1}{2}u_1^T(1+z_1^T P_\sigma)\left[\boldsymbol{D}'^2\delta(\boldsymbol{r}_1-\boldsymbol{r}_2) + \delta(\boldsymbol{r}_1-\boldsymbol{r}_2)\boldsymbol{D}^2\right] + u_2^T(1+z_2^T P_\sigma)\boldsymbol{D}'\cdot\delta(\boldsymbol{r}_1-\boldsymbol{r}_2)\boldsymbol{D}\Bigg\} \tag{9}$$

Now we calculate the potential energy density due to these terms within the Hartree-Fock approximation using a few useful properties. One reads

$$\left[\tau_z(1)+\tau_z(2)\right]P_\tau = \left[\tau_z(1)+\tau_z(2)\right]\frac{1+\boldsymbol{\tau}(1)\cdot\boldsymbol{\tau}(2)}{2} = \tau_z(1)+\tau_z(2). \tag{10}$$

Note that in the charge-independent terms the isospin exchange operator P_τ is present (and imposes a $\delta_{q_iq_j}$ in the Fock term). Now this will not be the case. The second property is

$$\tau_z(1)\tau_z(2)P_\tau = P_\tau \tag{11}$$

where we have neglected terms in $\tau_\pm$ since the expectation value in the HF ground state will be zero.

Charge symmetry breaking

For the charge symmetry breaking part, one finds for the antisymmetreized expectation value of the first term

$$\begin{aligned}\langle V^{s_0}_{\rm CSB}\rangle_{\rm AS} &= \frac{1}{2}\sum_{ij}\langle ij|V^{s_0}_{\rm CSB}(\boldsymbol{r}_1,\boldsymbol{r}_2)(1-P_xP_\tau P_\sigma)|ij\rangle \\ &= \frac{1}{8}\sum_{ij}\langle ij|\left[\tau_z(1)+\tau_z(2)\right]s_0(1+y_0P_\sigma)(1-P_\tau P_\sigma)|ij\rangle \\ &= \frac{1}{8}\sum_{ij}\langle ij|\left[\tau_z(1)+\tau_z(2)\right] \\ &\quad\times\left(s_0+s_0y_0P_\sigma - s_0P_\tau P_\sigma - s_0y_0P_\tau\right)|ij\rangle. \end{aligned}\tag{12}$$

Since Pauli spin matrices have zero trace,

$$\sum_i \phi_i^*(\boldsymbol{r},\sigma_1,q)\langle\sigma_1|\boldsymbol{\sigma}|\sigma_2\rangle\phi_i(\boldsymbol{r},\sigma_2,q) = 0,$$

Eq. (12) reads

$$\begin{aligned}\langle V^{s_0}_{\rm CSB}\rangle_{\rm AS} &= \frac{1}{8}\sum_{ij}\langle ij|\left[\tau_z(1)+\tau_z(2)\right] \\ &\quad\times\left(s_0+\frac{1}{2}s_0y_0 - \frac{1}{2}s_0P_\tau - s_0y_0P_\tau\right)|ij\rangle \\ &= \frac{s_0(1-y_0)}{16}\sum_{ij}\langle ij|\left[\tau_z(1)+\tau_z(2)\right]|ij\rangle \\ &= \frac{s_0(1-y_0)}{8}(\rho_n-\rho_p)(\rho_n+\rho_p) \\ &= \frac{s_0(1-y_0)}{8}(\rho_n^2-\rho_p^2).\end{aligned}$$

Eventually we have

$$\langle V^{s_0}_{\rm CSB}\rangle_{\rm AS} = \frac{s_0(1-y_0)}{8}(\rho_n^2-\rho_p^2). \tag{13}$$

From the variational principle we can write

$$\delta\langle H\rangle = \sum_q\int d\boldsymbol{r}\left[\frac{\hbar^2\delta\tau_q}{2m^*(\boldsymbol{r})} + U_q(\boldsymbol{r})\delta\rho_q + \boldsymbol{W}(\boldsymbol{r})\cdot\delta\boldsymbol{J}_q(\boldsymbol{r})\right], \tag{14}$$

where the mean field potential corresponding to Eq. (13) can be written as

$$U^{s_0,n}_{\rm CSB} = \frac{s_0(1-y_0)}{4}\rho_n,$$
$$U^{s_0,p}_{\rm CSB} = -\frac{s_0(1-y_0)}{4}\rho_p.$$

The results on the s_0 term are analogous to those published in Ref.[62].

In the second term $\boldsymbol{D}^2$ operators are symmetric to the exchange of spatial coordinates, that is, $\boldsymbol{D}^2P_x = \boldsymbol{D}^2$. Therefore

$$\begin{aligned}\langle V^{s_1}_{\rm CSB}\rangle_{\rm AS} &= \frac{1}{2}\sum_{ij}\langle ij|V^{s_1}_{\rm CSB}(\boldsymbol{r}_1,\boldsymbol{r}_2)(1-P_xP_\tau P_\sigma)|ij\rangle \\ &= \frac{1}{16}\sum_{ij}\langle ij|\left[\tau_z(1)+\tau_z(2)\right] \\ &\quad\times s_1(1+y_1P_\sigma)(1-P_xP_\tau P_\sigma)(\boldsymbol{D}'^2+\boldsymbol{D}^2)|ij\rangle.\end{aligned}\tag{15}$$

In Eq. (15), $\boldsymbol{D}'^2+\boldsymbol{D}^2$ can be substituted by $2\boldsymbol{D}^2$. In addition, terms in $\nabla_1^2\boldsymbol{\sigma}(2)$ or $\nabla_2^2\boldsymbol{\sigma}(1)$ will not contribute since $\sum_i\langle i|\boldsymbol{\sigma}|i\rangle = 0$. Then, we arrive eventually at

$$\begin{aligned}\langle V^{s_1}_{\rm CSB}\rangle_{\rm AS} &= -\frac{1}{64}\sum_{ij}\langle ij|\left[\tau_z(1)+\tau_z(2)\right] \\ &\quad\times s_1(1-y_1)\left[1-\boldsymbol{\sigma}(1)\cdot\boldsymbol{\sigma}(2)\right](\boldsymbol{\nabla}_1-\boldsymbol{\nabla}_2)^2|ij\rangle \\ &= -\frac{1}{64}\sum_{ij}\langle ij|\left[\tau_z(1)+\tau_z(2)\right]s_1(1-y_1) \\ &\quad\times(\boldsymbol{\nabla}_1^2+\boldsymbol{\nabla}_2^2-2\boldsymbol{\nabla}_1\cdot\boldsymbol{\nabla}_2)|ij\rangle \\ &\quad-\frac{1}{32}\sum_{ij}\langle ij|\left[\tau_z(1)+\tau_z(2)\right]s_1(1-y_1)\boldsymbol{\nabla}_1\cdot\boldsymbol{\nabla}_2\boldsymbol{\sigma}(1)\cdot\boldsymbol{\sigma}(2)|ij\rangle \\ &= -\frac{s_1(1-y_1)}{64}\Big[\rho\left(\nabla^2\rho_n-\nabla^2\rho_p\right) - 2\rho(\tau_n-\tau_p)\end{aligned}$$

$$+ (\rho_n - \rho_p)\nabla^2\rho - 2(\rho_n - \rho_p)\tau\Big] + \frac{s_1(1-y_1)}{64} \times [\boldsymbol{\nabla}\rho_n \cdot \boldsymbol{\nabla}\rho_n - \boldsymbol{\nabla}\rho_p \cdot \boldsymbol{\nabla}\rho_p] + \frac{s_1(1-y_1)}{32}\left[\boldsymbol{J}_n^2 - \boldsymbol{J}_p^2\right], \tag{16}$$

using the relations

1) $\nabla^2\rho = 2\sum_i \langle i|\nabla^2|i\rangle + 2\tau$;

2) $\sum_i \langle i|\boldsymbol{\nabla}|i\rangle = \frac{1}{2}\boldsymbol{\nabla}\rho$;

and the definition

3) $\boldsymbol{J}_q \equiv (-\imath)\sum_i \langle i|\boldsymbol{\nabla}\times\boldsymbol{\sigma}|i\rangle$ (in this case the sum over the index i does not include isospin for obvious reasons).

Noting that one can rewrite

$\int \boldsymbol{\nabla} f \cdot \boldsymbol{\nabla} f dV = \int \boldsymbol{\nabla}\cdot(f\boldsymbol{\nabla} f)\, dV - \int f\nabla^2 f dV$,

using the Gauss theorem

$\int \boldsymbol{\nabla} f \cdot \boldsymbol{\nabla} f dV = \int (f\boldsymbol{\nabla} f)\cdot d\boldsymbol{S} - \int f\nabla^2 f dV$,

considering f is a well behaved function of the spatial coordinates that goes to zero at infinity, and being S a surface enclosing the whole space V, then,

$\int \boldsymbol{\nabla} f \cdot \boldsymbol{\nabla} f dV = -\int f\nabla^2 f dV$,

we can write the final expression

$$\begin{aligned}
&\langle V^{s_1}_{\rm CSB}\rangle_{\rm AS} \\
&= -\frac{s_1(1-y_1)}{32}\Bigg[\rho_n\nabla^2\rho_n - \rho_p\nabla^2\rho_p - 2(\rho_n\tau_n - \rho_p\tau_p) \\
&\qquad + \frac{1}{2}\left(\rho_n\nabla^2\rho_n - \rho_p\nabla^2\rho_p\right) - \left(\boldsymbol{J}_n^2 - \boldsymbol{J}_p^2\right)\Bigg] \\
&= \frac{s_1(1-y_1)}{32}\Bigg[-\frac{3}{2}\rho_n\nabla^2\rho_n + \frac{3}{2}\rho_p\nabla^2\rho_p \\
&\qquad + 2(\rho_n\tau_n - \rho_p\tau_p) + \left(\boldsymbol{J}_n^2 - \boldsymbol{J}_p^2\right)\Bigg].
\end{aligned} \tag{17}$$

The mean field potential corresponding to Eq. (17) can be written as follows,

$$\begin{aligned}
\frac{\hbar^2}{2m_n^*(\boldsymbol{r})} &= \frac{\hbar^2}{2m_{n0}^*(\boldsymbol{r})} + \frac{s_1(1-y_1)}{16}\rho_n, \\
\frac{\hbar^2}{2m_p^*(\boldsymbol{r})} &= \frac{\hbar^2}{2m_{p0}^*(\boldsymbol{r})} - \frac{s_1(1-y_1)}{16}\rho_p, \\
U^{s_1,n}_{\rm CSB} &= -\frac{3}{32}s_1(1-y_1)\nabla^2\rho_n + \frac{s_1(1-y_1)}{16}\tau_n, \\
U^{s_1,p}_{\rm CSB} &= \frac{3}{32}s_1(1-y_1)\nabla^2\rho_p - \frac{s_1(1-y_1)}{16}\tau_p, \\
\boldsymbol{W}^{s_1,n}_{\rm CSB} &= \frac{s_1(1-y_1)}{16}\boldsymbol{J}_n, \\
\boldsymbol{W}^{s_1,p}_{\rm CSB} &= -\frac{s_1(1-y_1)}{16}\boldsymbol{J}_p,
\end{aligned}$$

where we have used the relation $\frac{\delta}{\delta\rho_q}\left(\rho_q\nabla^2\rho_q\right) = 2\nabla^2\rho_q$. The term $\hbar^2/2m_{n0}^*(\boldsymbol{r})$ in the effective mass comes from the momentum dependent terms t_1 and t_2 of Skyrme interaction.

Now the third term, where $\boldsymbol{D}'\cdot\boldsymbol{D}P_x = -\boldsymbol{D}'\cdot\boldsymbol{D}$, becomes

$$\begin{aligned}
\langle V^{s_2}_{\rm CSB}\rangle_{\rm AS} &= \frac{1}{2}\sum_{ij}\langle ij|V^{s_2}_{\rm CSB}(\boldsymbol{r}_1,\boldsymbol{r}_2)(1 - P_xP_\tau P_\sigma)|ij\rangle \\
&= \frac{1}{8}\sum_{ij}\langle ij|\left[\tau_z(1) + \tau_z(2)\right] \\
&\qquad \times s_2(1 + y_2P_\sigma)(1 + P_\tau P_\sigma)(\boldsymbol{D}'\cdot\boldsymbol{D})|ij\rangle, \\
&= \frac{1}{32}\sum_{ij}\langle ij|\left[\tau_z(1) + \tau_z(2)\right] \\
&\qquad \times s_2(1 + y_2)\frac{3 + \boldsymbol{\sigma}(1)\cdot\boldsymbol{\sigma}(2)}{2}(\boldsymbol{\nabla}_1' - \boldsymbol{\nabla}_2')(\boldsymbol{\nabla}_1 - \boldsymbol{\nabla}_2)|ij\rangle, \\
&= \frac{1}{32}\sum_{ij}\langle ij|\left[\tau_z(1) + \tau_z(2)\right] \\
&\qquad \times s_2(1 + y_2)\left[3 + \boldsymbol{\sigma}(1)\cdot\boldsymbol{\sigma}(2)\right](\boldsymbol{\nabla}_1'\cdot\boldsymbol{\nabla}_1 - \boldsymbol{\nabla}_2'\cdot\boldsymbol{\nabla}_1)|ij\rangle.
\end{aligned} \tag{18}$$

Due to symmetry in the term $(\boldsymbol{\nabla}_1' - \boldsymbol{\nabla}_2')(\boldsymbol{\nabla}_1 - \boldsymbol{\nabla}_2)$ in exchanging particles 1 and 2, we can write it as $2\boldsymbol{\nabla}_1'\cdot\boldsymbol{\nabla}_1 - 2\boldsymbol{\nabla}_2'\cdot\boldsymbol{\nabla}_1$, which is further transformed by integrating by parts and taking into account that $\nabla_1^2\boldsymbol{\sigma}(2)$ or $\boldsymbol{\nabla}_1'\cdot\boldsymbol{\nabla}_1\boldsymbol{\sigma}(2)$ will not contribute since $\sum_i\langle i|\boldsymbol{\sigma}|i\rangle = 0$. Eventually

$$\begin{aligned}
\langle V^{s_2}_{\rm CSB}\rangle_{\rm AS} &= \frac{1}{32}\sum_{ij}\langle ij|\left[\tau_z(1) + \tau_z(2)\right]s_2(1 + y_2) \\
&\quad \times\left[3 + \boldsymbol{\sigma}(1)\cdot\boldsymbol{\sigma}(2)\right](2\boldsymbol{\nabla}_1'\cdot\boldsymbol{\nabla}_1 + \nabla_1^2 + \boldsymbol{\nabla}_1\cdot\boldsymbol{\nabla}_2)|ij\rangle \\
&= \frac{3}{32}s_2(1 + y_2)\sum_{ij}\langle ij|\left[\tau_z(1) + \tau_z(2)\right] \\
&\qquad \times(2\boldsymbol{\nabla}_1'\cdot\boldsymbol{\nabla}_1 + \nabla_1^2 + \boldsymbol{\nabla}_1\cdot\boldsymbol{\nabla}_2)|ij\rangle \\
&+ \frac{1}{32}s_2(1 + y_2)\sum_{ij}\langle ij|\left[\tau_z(1) + \tau_z(2)\right]\boldsymbol{\sigma}(1)\cdot\boldsymbol{\sigma}(2)\boldsymbol{\nabla}_1\cdot\boldsymbol{\nabla}_2|ij\rangle \\
&= \frac{3}{32}s_2(1 + y_2)\Bigg[2(\tau_n - \tau_p)\rho + 2\tau(\rho_n - \rho_p) + \frac{1}{2}\rho\nabla^2(\rho_n - \rho_p) \\
&- \rho(\tau_n - \tau_p) + \frac{1}{2}(\rho_n - \rho_p)\nabla^2\rho - \tau(\rho_n - \rho_p) \\
&+ \frac{1}{2}\boldsymbol{\nabla}(\rho_n - \rho_p)\cdot\boldsymbol{\nabla}(\rho_n + \rho_p) - \frac{1}{3}(\boldsymbol{J}_n - \boldsymbol{J}_p)(\boldsymbol{J}_n + \boldsymbol{J}_p)\Bigg] \\
&= \frac{3}{32}s_2(1 + y_2)\Bigg[2(\tau_n\rho_n - \tau_p\rho_p) + \rho_n\nabla^2\rho_n - \rho_p\nabla^2\rho_p \\
&\qquad - \frac{1}{2}(\rho_n\nabla^2\rho_n - \rho_p\nabla^2\rho_p) - \frac{1}{3}(\boldsymbol{J}_n^2 - \boldsymbol{J}_p^2)\Bigg].
\end{aligned}$$

Then the s_2 terms read

$$\begin{aligned}
\langle V^{s_2}_{\rm CSB}\rangle_{\rm AS} &= \frac{3}{32}s_2(1 + y_2)\Bigg[2(\tau_n\rho_n - \tau_p\rho_p) \\
&\quad + \frac{1}{2}(\rho_n\nabla^2\rho_n - \rho_p\nabla^2\rho_p) - \frac{1}{3}(\boldsymbol{J}_n^2 - \boldsymbol{J}_p^2)\Bigg].
\end{aligned} \tag{19}$$

The mean field potential corresponding to Eq. (19) can be written as follows,

$$\begin{aligned}
\frac{\hbar^2}{2m_n^*(\boldsymbol{r})} &= \frac{\hbar^2}{2m_{n0}^*(\boldsymbol{r})} + \frac{3}{16}s_2(1+y_2)\rho_n, \\
\frac{\hbar^2}{2m_p^*(\boldsymbol{r})} &= \frac{\hbar^2}{2m_{p0}^*(\boldsymbol{r})} - \frac{3}{16}s_2(1+y_2)\rho_p, \\
U_{\rm CSB}^{s_2,n} &= \frac{3}{32}s_2(1+y_2)\left(2\tau_n + \nabla^2\rho_n\right), \\
U_{\rm CSB}^{s_2,p} &= -\frac{3}{32}s_2(1+y_2)\left(2\tau_p + \nabla^2\rho_p\right), \\
\boldsymbol{W}_{\rm CSB}^{s_2,n} &= -\frac{1}{16}s_2(1+y_2)\boldsymbol{J}_n, \\
\boldsymbol{W}_{\rm CSB}^{s_2,p} &= +\frac{1}{16}s_2(1+y_2)\boldsymbol{J}_p.
\end{aligned}$$

Charge independence breaking

For the charge independence breaking part, assuming there is no isospin-charge mixing in the Hartree-Fock states ($P_\tau \to \delta_{q_iq_j}$), one can find for the first term:

$$\begin{aligned}
\langle V_{\rm CIB}^{u_0}\rangle_{\rm AS} &= \frac{1}{2}\sum_{ij}\langle ij|V_{\rm CIB}^{u_0}(\boldsymbol{r}_1,\boldsymbol{r}_2)(1-P_xP_\tau P_\sigma)|ij\rangle \\
&= \frac{1}{4}\sum_{ij}\langle ij|\tau_z(1)\tau_z(2)u_0(1+z_0P_\sigma)(1-P_xP_\tau P_\sigma)|ij\rangle \\
&= \frac{1}{4}\sum_{ij}\langle ij|\tau_z(1)\tau_z(2)\left(u_0+u_0z_0P_\sigma-u_0P_\tau P_\sigma-u_0z_0P_\tau\right)|ij\rangle \\
&= \frac{1}{4}\sum_{ij}\langle ij|\tau_z(1)\tau_z(2)\left(u_0+\frac{1}{2}u_0z_0-\frac{1}{2}u_0P_\tau-u_0z_0P_\tau\right)|ij\rangle \\
&= \frac{1}{8}\sum_{ij}\langle ij|\left[u_0(2+z_0)\tau_z(1)\tau_z(2)-u_0(2z_0+1)P_\tau\right]|ij\rangle \\
&= \frac{1}{8}\sum_{ij}\langle ij|\left[u_0(2+z_0)\tau_z(1)\tau_z(2)-u_0(2z_0+1)\delta_{q_iq_j}\right]|ij\rangle \\
&= \frac{1}{8}\left[u_0(2+z_0)(\rho_n-\rho_p)^2-u_0(1+2z_0)(\rho_n^2+\rho_p^2)\right].
\end{aligned}$$

The u_0 terms give

$$\langle V_{\rm CIB}^{u_0}\rangle_{\rm AS} = \frac{1}{8}\left[u_0(1-z_0)(\rho_n^2+\rho_p^2)-2u_0(2+z_0)\rho_n\rho_p\right]. \tag{21}$$

The isotensor CIB interaction (9) gives another form to the EDF, namely

$$\langle V_{\rm CIB^T}^{u_0^T}\rangle_{\rm AS} = \frac{1}{4}\left[u_0^T(1-z_0^T)(\rho_n-\rho_p)^2\right]. \tag{22}$$

Here, it is clear why this type of interaction does not contribute to the equation of state of symmetric nuclear matter while that in Eq.(21) does. The mean field potential corresponding to Eq. (21) can be written as

$$\begin{aligned}
U_{\rm CIB}^{u_0,n} &= \frac{1}{4}\left[u_0(1-z_0)\rho_n-u_0(2+z_0)\rho_p\right], \\
U_{\rm CIB}^{u_0,p} &= \frac{1}{4}\left[u_0(1-z_0)\rho_p-u_0(2+z_0)\rho_n\right].
\end{aligned}$$

The term in u_1 can be treated in analogy with that of s_1,

$$\begin{aligned}
\langle V_{\rm CIB}^{u_1}\rangle_{\rm AS} &= \frac{1}{2}\sum_{ij}\langle ij|V_{\rm CIB}^{u_1}(\boldsymbol{r}_1,\boldsymbol{r}_2)(1-P_xP_\tau P_\sigma)|ij\rangle \\
&= \frac{1}{8}\sum_{ij}\langle ij|\tau_z(1)\tau_z(2) \\
&\quad \times u_1(1+z_1P_\sigma)(1-P_xP_\tau P_\sigma)(\mathbf{D'}^2+\mathbf{D}^2)|ij\rangle \\
&= \frac{1}{8}\sum_{ij}\langle ij|\tau_z(1)\tau_z(2) \\
&\quad \times\left(u_1+u_1z_1P_\sigma-u_1P_\tau P_\sigma-u_1z_1P_\tau\right)(\mathbf{D'}^2+\mathbf{D}^2)|ij\rangle \\
&= -\frac{1}{32}\sum_{ij}\langle ij|\Big\{\Big[u_1(2+z_1)\tau_z(1)\tau_z(2) \\
&\quad - u_1(1+2z_1)\delta_{q_iq_j}\Big](\boldsymbol{\nabla}_1^2+\boldsymbol{\nabla}_2^2-2\boldsymbol{\nabla}_1\boldsymbol{\nabla}_2) \\
&\quad - 2\left[u_1z_1\tau_z(1)\tau_z(2)-u_1\delta_{q_iq_j}\right]\boldsymbol{\sigma}(1)\boldsymbol{\sigma}(2)\boldsymbol{\nabla}_1\boldsymbol{\nabla}_2\Big\}|ij\rangle.
\end{aligned}$$

Finally we have the EDF for u_1 terms as

$$\begin{aligned}
\langle V_{\rm CIB}^{u_1}\rangle_{\rm AS} = \frac{1}{32}\Big\{ &-\frac{3}{2}u_1(1-z_1)\left(\rho_n\nabla^2\rho_n+\rho_p\nabla^2\rho_p\right) \\
&+\frac{3}{2}u_1(2+z_1)\left(\rho_n\nabla^2\rho_p+\rho_p\nabla^2\rho_n\right) \\
&+2u_1(1-z_1)\left(\tau_n\rho_n+\tau_p\rho_p\right)-2u_1(2+z_1)\left(\tau_n\rho_p+\tau_p\rho_n\right) \\
&+u_1(1-z_1)\left(\boldsymbol{J}_n^2+\boldsymbol{J}_p^2\right)+2u_1z_1\boldsymbol{J}_n\boldsymbol{J}_p\Big\},
\end{aligned}$$

where we have used the relation,

$$\begin{aligned}
\int\boldsymbol{\nabla}f_1\cdot\boldsymbol{\nabla}f_2dV &= \frac{1}{2}\int\boldsymbol{\nabla}f_1\cdot\boldsymbol{\nabla}f_2dV+\frac{1}{2}\int\boldsymbol{\nabla}f_2\cdot\boldsymbol{\nabla}f_1dV \\
&= \frac{1}{2}\int\boldsymbol{\nabla}\cdot\left(f_1\boldsymbol{\nabla}f_2\right)dV-\frac{1}{2}\int f_1\nabla^2f_2dV \\
&\quad +\frac{1}{2}\int\boldsymbol{\nabla}\cdot\left(f_2\boldsymbol{\nabla}f_1\right)dV-\frac{1}{2}\int f_2\nabla^2f_1dV\ ,
\end{aligned} \tag{20}$$

recalling again the Gauss theorem

$$\int\boldsymbol{\nabla}f_1\cdot\boldsymbol{\nabla}f_2dV = -\frac{1}{2}\int\left(f_1\nabla^2f_2+f_2\nabla^2f_1\right)dV\ . \tag{23}$$

The mean field potential corresponding to this piece can be written as

$$\frac{\hbar^2}{2m_n^*(\boldsymbol{r})} = \frac{\hbar^2}{2m_{n0}^*(\boldsymbol{r})} + \frac{1}{16}\left[u_1(1-z_1)\rho_n-u_1(2+z_1)\rho_p\right],$$

$$\frac{\hbar^2}{2m_p^*(\boldsymbol{r})} = \frac{\hbar^2}{2m_{p0}^*(\boldsymbol{r})} + \frac{1}{16}\left[u_1(1-z_1)\rho_p - u_1(2+z_1)\rho_n\right],$$
$$U_{\rm CIB}^{u_1,n} = \frac{1}{32}\left[-3u_1(1-z_1)\nabla^2\rho_n + 3u_1(2+z_1)\nabla^2\rho_p + 2u_1(1-z_1)\tau_n - 2u_1(2+z_1)\tau_p\right],$$
$$U_{\rm CIB}^{u_1,p} = \frac{1}{32}\left[-3u_1(1-z_1)\nabla^2\rho_p + 3u_1(2+z_1)\nabla^2\rho_n + 2u_1(1-z_1)\tau_p - 2u_1(2+z_1)\tau_n\right],$$
$$\boldsymbol{W}_{\rm CIB}^{u_1,n} = \frac{1}{16}\left[u_1(1-z_1)\boldsymbol{J}_n + u_1 z_1 \boldsymbol{J}_p\right],$$
$$\boldsymbol{W}_{\rm CIB}^{u_1,p} = \frac{1}{16}\left[u_1(1-z_1)\boldsymbol{J}_p + u_1 z_1 \boldsymbol{J}_n\right].$$

The term in u_2 can be evaluated as follows:

$$\langle V_{\rm CIB}^{u_2}\rangle_{\rm AS} = \frac{1}{2}\sum_{ij}\langle ij|V_{\rm CIB}^{u_2}(\boldsymbol{r}_1,\boldsymbol{r}_2)(1-P_xP_\tau P_\sigma)|ij\rangle$$
$$= \frac{1}{4}\sum_{ij}\langle ij|\tau_z(1)\tau_z(2) \times u_2(1+z_2P_\sigma)(1-P_xP_\tau P_\sigma)\boldsymbol{D}'\cdot\boldsymbol{D}|ij\rangle$$
$$= \frac{1}{4}\sum_{ij}\langle ij|\tau_z(1)\tau_z(2)\Big(u_2 + u_2z_2P_\sigma + u_2P_\tau P_\sigma + u_2z_2P_\tau\Big)\boldsymbol{D}'\cdot\boldsymbol{D}|ij\rangle$$
$$= \frac{1}{16}\Bigg[\frac{3}{4}u_2(1+z_2)\left(\rho_n\nabla^2\rho_n + \rho_p\nabla^2\rho_p\right) - \frac{1}{4}u_2(2+z_2)\left(\rho_p\nabla^2\rho_n + \rho_p\nabla^2\rho_n\right) + 3u_2(1+z_2)\left(\tau_n\rho_n + \tau_p\rho_p\right) - u_2(2+z_2)\left(\tau_n\rho_p + \tau_p\rho_n\right) - \frac{1}{2}u_2(1+z_2)\left(\boldsymbol{J}_n^2 + \boldsymbol{J}_p^2\right) + u_2z_2\boldsymbol{J}_n\boldsymbol{J}_p\Bigg].$$

The u_2 terms are thus summarized as follows,

$$\langle V_{\rm CIB}^{u_2}\rangle_{\rm AS} = \frac{1}{16}\Bigg[\frac{3}{4}u_2(1+z_2)\left(\rho_n\nabla^2\rho_n + \rho_p\nabla^2\rho_p\right) - \frac{1}{4}u_2(2+z_2)\left(\rho_p\nabla^2\rho_n + \rho_p\nabla^2\rho_n\right) + 3u_2(1+z_2)\left(\tau_n\rho_n + \tau_p\rho_p\right) - u_2(2+z_2)\left(\tau_n\rho_p + \tau_p\rho_n\right) - \frac{1}{2}u_2(1+z_2)\left(\boldsymbol{J}_n^2 + \boldsymbol{J}_p^2\right) + u_2z_2\boldsymbol{J}_n\boldsymbol{J}_p\Bigg].$$

The mean field potential corresponding to this piece can be written as

$$\frac{\hbar^2}{2m_n^*(\boldsymbol{r})} = \frac{\hbar^2}{2m_{n0}^*(\boldsymbol{r})} + \frac{3}{16}u_2(1+z_2)\rho_n - \frac{1}{16}u_2(2+z_2)\rho_p,$$
$$\frac{\hbar^2}{2m_p^*(\boldsymbol{r})} = \frac{\hbar^2}{2m_{p0}^*(\boldsymbol{r})} + \frac{3}{16}u_2(1+z_2)\rho_p - \frac{1}{16}u_2(2+z_2)\rho_n,$$
$$U_{\rm CIB}^{u_2,n} = \frac{3}{32}u_2(1+z_2)\left(\nabla^2\rho_n + 2\tau_n\right) - \frac{1}{32}u_2(2+z_2)\left(\nabla^2\rho_p + 2\tau_p\right),$$
$$U_{\rm CIB}^{u_2,p} = \frac{3}{32}u_2(1+z_2)\left(\nabla^2\rho_p + 2\tau_p\right) - \frac{1}{32}u_2(2+z_2)\left(\nabla^2\rho_n + 2\tau_n\right),$$
$$\boldsymbol{W}_{\rm CIB}^{u_2,n} = -\frac{1}{16}u_2(1+z_2)\boldsymbol{J}_n + \frac{1}{16}u_2z_2\boldsymbol{J}_p,$$
$$\boldsymbol{W}_{\rm CIB}^{u_2,p} = -\frac{1}{16}u_2(1+z_2)\boldsymbol{J}_p + \frac{1}{16}u_2z_2\boldsymbol{J}_n.$$

where we have used $\frac{\delta}{\delta f_1}\left(f_1\nabla^2 f_2 + f_2\nabla^2 f_1\right) = 2\nabla^2 f_2$.

Summary

Finally, we can write the total energy density associated with the CSB terms as:

$$\mathcal{H}_{\rm CSB} = \frac{s_0(1-y_0)}{8}(\rho_n^2-\rho_p^2) + \frac{s_1(1-y_1)}{32}\Big[-\frac{3}{2}\rho_n\nabla^2\rho_n + \frac{3}{2}\rho_p\nabla^2\rho_p + 2(\rho_n\tau_n - \rho_p\tau_p) + \left(\boldsymbol{J}_n^2 - \boldsymbol{J}_p^2\right)\Big] + \frac{3}{32}s_2(1+y_2)\Bigg[2(\tau_n\rho_n - \tau_p\rho_p) + \frac{1}{2}(\rho_n\nabla^2\rho_n - \rho_p\nabla^2\rho_p) - \frac{1}{3}(\boldsymbol{J}_n^2 - \boldsymbol{J}_p^2)\Bigg], \tag{24}$$

and the total mean field potentials as:

$$\frac{\hbar^2}{2m_n^*(\boldsymbol{r})} = \frac{\hbar^2}{2m_{n0}^*(\boldsymbol{r})} + \frac{s_1(1-y_1)}{16}\rho_n + \frac{3}{16}s_2(1+y_2)\rho_n,$$
$$\frac{\hbar^2}{2m_p^*(\boldsymbol{r})} = \frac{\hbar^2}{2m_{p0}^*(\boldsymbol{r})} - \frac{s_1(1-y_1)}{16}\rho_p - \frac{3}{16}s_2(1+y_2)\rho_p,$$
$$U_{\rm CSB}^{n} = \frac{s_0(1-y_0)}{4}\rho_n - \frac{3}{32}s_1(1-y_1)\nabla^2\rho_n + \frac{s_1(1-y_1)}{16}\tau_n + \frac{3}{32}s_2(1+y_2)\left(2\tau_n + \nabla^2\rho_n\right),$$
$$U_{\rm CSB}^{p} = -\frac{s_0(1-y_0)}{4}\rho_p + \frac{3}{32}s_1(1-y_1)\nabla^2\rho_p - \frac{s_1(1-y_1)}{16}\tau_p - \frac{3}{32}s_2(1+y_2)\left(2\tau_p + \nabla^2\rho_p\right),$$
$$\boldsymbol{W}_{\rm CSB}^{n} = \frac{s_1(1-y_1)}{16}\boldsymbol{J}_n - \frac{1}{16}s_2(1+y_2)\boldsymbol{J}_n,$$
$$\boldsymbol{W}_{\rm CSB}^{p} = -\frac{s_1(1-y_1)}{16}\boldsymbol{J}_p + \frac{1}{16}s_2(1+y_2)\boldsymbol{J}_p. \tag{25}$$

We can also write the total energy density associated with the CIB terms as

$$\mathcal{H}_{\rm CIB} = \frac{1}{8}\left[u_0(1-z_0)(\rho_n^2+\rho_p^2) - 2u_0(2+z_0)\rho_n\rho_p\right] + \frac{1}{32}\Bigg\{-\frac{3}{2}u_1(1-z_1)\left(\rho_n\nabla^2\rho_n + \rho_p\nabla^2\rho_p\right) + \frac{3}{2}u_1(2+z_1)\left(\rho_n\nabla^2\rho_p + \rho_p\nabla^2\rho_n\right) + 2u_1(1-z_1)\left(\tau_n\rho_n + \tau_p\rho_p\right) - 2u_1(2+z_1)\left(\tau_n\rho_p + \tau_p\rho_n\right) + u_1(1-z_1)\left(\boldsymbol{J}_n^2 + \boldsymbol{J}_p^2\right) + 2u_1z_1\boldsymbol{J}_n\boldsymbol{J}_p\Bigg\}$$

$$+\frac{1}{16}\Bigg[\frac{3}{4}u_2(1+z_2)\left(\rho_n\nabla^2\rho_n+\rho_p\nabla^2\rho_p\right)$$
$$-\frac{1}{4}u_2(2+z_2)\left(\rho_p\nabla^2\rho_n+\rho_p\nabla^2\rho_n\right)$$
$$+3u_2(1+z_2)\left(\tau_n\rho_n+\tau_p\rho_p\right)-u_2(2+z_2)\left(\tau_n\rho_p+\tau_p\rho_n\right)$$
$$-\frac{1}{2}u_2(1+z_2)\left(\boldsymbol{J}_n^2+\boldsymbol{J}_p^2\right)+u_2z_2\boldsymbol{J}_n\boldsymbol{J}_p\Bigg], \tag{26}$$

and the total mean field potentials as

$$\frac{\hbar^2}{2m_n^*(\boldsymbol{r})}=\frac{\hbar^2}{2m_{n0}^*(\boldsymbol{r})}$$
$$+\frac{1}{32}\left[-2u_1(4+5z_1)\rho+2u_1(5+4z_1)\rho_n\right]$$
$$+\frac{3}{16}u_2(1+z_2)\rho_n+\frac{3}{16}u_2z_2\rho_p,$$
$$\frac{\hbar^2}{2m_p^*(\boldsymbol{r})}=\frac{\hbar^2}{2m_{p0}^*(\boldsymbol{r})}$$
$$+\frac{1}{32}\left[-2u_1(4+5z_1)\rho+2u_1(5+4z_1)\rho_p\right]$$
$$+\frac{3}{16}u_2(1+z_2)\rho_p+\frac{3}{16}u_2z_2\rho_n,$$
$$U_{\rm CIB}^n=\frac{1}{4}\left[u_0(1-z_0)\rho_n-(4u_0+5u_0z_0)\rho_p\right]+$$
$$\frac{1}{32}\left[u_1(4+5z_1)\left(3\nabla^2\rho-2\tau\right)-u_1(5+4z_1)\left(3\nabla^2\rho_n-2\tau_n\right)\right]$$
$$+\frac{3}{16}u_2(1+z_2)\left(\tau_n+\frac{1}{2}\nabla^2\rho_n\right)+\frac{3}{16}u_2z_2\left(\tau_p+\frac{1}{2}\nabla^2\rho_p\right),$$
$$U_{\rm CIB}^p\frac{1}{4}\left[u_0(1-z_0)\rho_p-(4u_0+5u_0z_0)\rho_n\right]$$
$$+\frac{1}{32}\left[u_1(4+5z_1)\left(3\nabla^2\rho-2\tau\right)-u_1(5+4z_1)\left(3\nabla^2\rho_p-2\tau_p\right)\right]$$
$$+\frac{3}{16}u_2(1+z_2)\left(\tau_p+\frac{1}{2}\nabla^2\rho_p\right)+\frac{3}{16}u_2z_2\left(\tau_n+\frac{1}{2}\nabla^2\rho_n\right),$$
$$\boldsymbol{W}_{\rm CIB}^n=\frac{1}{16}\Bigg[u_1(1-z_1)\boldsymbol{J}_n+u_1(2+z_1)\boldsymbol{J}_p$$
$$-u_2(1+z_2)\boldsymbol{J}_n-u_2(2-z_2)\boldsymbol{J}_p\Bigg],$$
$$\boldsymbol{W}_{\rm CIB}^p=\frac{1}{16}\Bigg[u_1(1-z_1)\boldsymbol{J}_p$$
$$+u_1(2+z_1)\boldsymbol{J}_n-u_2(1+z_2)\boldsymbol{J}_p-u_2(2-z_2)\boldsymbol{J}_n\Bigg].$$

References

1. A. Bohr and B. R. Mottelson, *Nuclear Structure* (World Scientific, 1969), Vol. I.
2. N Auerbach, J Hfner, AK Kerman, and CM Shakin, Reviews of Modern Physics 44 (1), 48 (1972).
3. M. N. Harakeh and A. Woude, "Giant Resonances: fundamental high-frequency modes of nuclear excitation" (Oxford University Press, London, 2001).
4. M. Ichimura, H. Sakai and Wakasa, Prog. Part. Nucl. Phys. **56**, 446 (2006).
5. A. Arima , K. Shimizu, W. Bentz and H. Hyuga, Adv. Nucl. Phys. **18**, 1 (1987).
6. I. S. Towner, Phys. Rep. **155**, 263 (1987).
7. C. Gaarde et al., Nucl. Phys. A **369** 258 (1981).
8. T. Wakasa et al., Phys. Rev. C **55**, 2909 (1997).
9. K. Yako et al., Phys. Lett. B **615**, 193(2005).
10. K. Yako et al., Phys. Rev. Lett. **103**, 012503 (2009).
11. M. Sasano, *et al.*, Phys. Rev. Lett. **107**, 202501 (2011); M. Sasano et al., Phys. Rev. C **86**, 034324 (2012).
12. T. Wakasa et al., Phys. Rev. C **85**, 064606 (2012).
13. F. T. Avignone, III, S. R. Elliott and J. Engel, Rev. Mod. Phys. **80**, 481 (2008).
14. S. Fantoni et al., Phys. Rev. Lett. 87, 181101 (2001); G. Shen et al., Phys. Rev. C87, 025802 (2013).
15. T. Suzuki et al., Phys. Rev. C **74**, 034307 (2006).
16. C. Shen, U. Lombardo, N. Van Giai, and W. Zuo, Phys. Rev. 68, 055802 (2003).
17. J. Margueron, I. Vidaña, and I. Bombaci, Phys. Rev. C68, 055806 (2003).
18. K. Langanke et al., Phys. Rev. Lett. 93, 202501 (2004); 100, 011101 (2008).
19. H. Toki et al., Phys. Rev. C **88**, 015806 (2013).
20. S. Jones et al., The Astrophys. J. **772**, 150 (2013).
21. T. Suzuki, H. Toki and K. Nomoto, The Astrophys. J. **817**, 163 (2016).
22. S. Reddy et al., Phys. Rev. C **59**, 2888(1999); A. Burrows and R. F. Sawyer, Phys. Rev. C **58**, 554 (1998).
23. A. Radhi et al., Phys. Rev. C **91**, 045803(2015).
24. G. Bertsch and I. Hamamoto, Phys. Rev. C **26**, 1323(1982).
25. A. Bohr and B. R. Mottelson, Phys. Lett. B **100**, 10 (1981).
26. M. Rho, Nucl. Phys. A **231**, 493 (1974); E. Oset and M. Rho, Phys. Rev. Lett. **42**, 47 (1979).
27. C. L. Bai, H. Q. Zhang, X. Z. Zhang, F. R. Xu, H. Sagawa, and G. Colò, Phys. Rev. C **79**, 0411301(R) (2009).
28. A. Arima, in *Proceedings of the International Symposium on New Facet of Spin Giant Resonances in Nuclei, 1997*, edited by H. Sakai, H. Okamura, and T. Wakasa (Univ. of Tokyo, Japan, 1997), p. 3.
29. W. G. Love and M. A. Franey, Phys. Rev. C **24**, 1073 (1981).
30. H. Matsubara et al., Phys. Rev. Lett. **115**, 102501 (2015) and private communications.
31. C.L. Bai, H. Sagawa, M. Sasano, T. Uesaka, K. Hagino, H.Q. Zhang, X.Z. Zhang, and F.R. Xu, Phys. Lett. B **719**, 116 (2013).
32. Y. Fujita *et al.*, Phys. Rev. Lett. **112**, 112502 (2014).
33. Y. Tanimura, H. Sagawa and K. Hagino, Prog. Theor. Exp. Phys. 053D02 (2014).
34. H. Sagawa, C.L. Bai and G. Colò, (2016) Physica Scripta the '75 Nobel Prize celebration volume(2016) in press.
35. S. J. Q. Robinson and L. Zamick, Phys. Rev. C **66**, 034303 (2002).
36. P. Van Isacker, J. Engel and K. Nomura, Phys. Rev. C **96**, 064305 (2017).
37. M. Takaki, T. Uesaka et al., Proposal for experiment at RCNP, "Search for double Gamow Teller giant resonances in ^{48}Ti via the heavy-ion double charge exchange ^{48}Ca(^{12}C, ^{12}Be(0_2^+)) reaction" (2015).
38. F. Cappuzzello, C. Agodi, M. Bondi, D. Carbone, M. Cavallaro, A. Foti, Journal of Physics: Conference Series 630, 012018 (2015).

39. S. Mordechai and C.F. Moore, Nature 352, 393 (1991)
40. H. Ward et al. , Phys. Rev. Lett. 70, 3209 (1993)
41. Ph. Chomaz and N. Frascaria, Phys. Rep. 252, 275 (1995).
42. J. Blomgren et al., Phys. Lett. B362, 34 (1995).
43. T. Uesaka, M. Takaki et al., Proposal for Nuclear Physics Experiment at RI Beam Factory " Search for Double Gamow-Teller Giant Resonances in $\beta\beta-$decay nuclei via the heavy-ion double charge exchange^{48}Ca(^{12}C, ^{12}Be(0_2^+)) reaction" (2016).
44. N. Shimizu, J. Menéndez, and K. Yako Phys. Rev. Lett. 120, 142502 (2018)
45. P. Vogel, M. Ericson and J. D. Vergados, Phys. Lett. B212, 259(1988).
46. D. C. Zheng, L. Zamick and N. Auerbach, Phys. Rev. C40, 936 (1989).
47. K. Muto, Phys. Lett. B277, 13 (1992).
48. H. Sagawa and T. Uesaka, Phys. Rev. C94, 064325 (2016)
49. G. Colò, N. Van Giai, P.F. Bortignon, R.A. Broglia, Phys. Rev. C50 (1994) 1496.
50. G. Colò, H. Sagawa, N. Van Giai, P.F. Bortignon and T. Suzuki, Phys. Rev. C57 (1998) 3049.
51. Y.F. Niu, G. Colo, M. Brenna, P.F. Bortignon, and J. Meng, Phys. Rev. C 85, 034313 (2012).
52. M. Oertel, M. Hempel, T. Klähn, S. Typel, Rev. Mod. Phys. 89, 015007 (2017).
53. J.M. Lattimer and Y. Lin, Astr. J. 771, 51 (2013).
54. B.A. Li and X. Han, Phys. Lett. B727, 276 (2013).
55. C.J. Horowitz, et al., J. Phys. G: Nuclear and Particle Physics, 41, 093001 (2014).
56. B.A. Brown, Phys. Rev. Lett. 85, 5296 (2000).
57. X. Roca-Maza, G. Colò, and H. Sagawa, Phys. Rev. C86, 031306 (2012).
58. X. Roca-Maza, G. Colò, H. Sagawa, Phys. Rev. Lett. 120, 202501 (2018).
59. N. Auerbach et al., Phys. Rev. Lett. 23, 484 (1969).
60. T. Suzuki, H. Sagawa, and N. Van Giai, Phys. Rev. C 47 (1993) R1360
61. H. Sagawa, N. V. Giai, and T. Suzuki, Physics Letters B 353, 7 (1995).
62. P. Baczyk, J.Dobaczewski, M.Konieczka, W.Satula, T.Nakatsukasa, and K.Sato. Physics Letters B778, 178(2018).
63. H. Müther, A. Polls, R. Machleidt, Phys. Lett. B 445, 259 (1999).
64. J. Yasuda, M. Sasano, R.G.T. Zegers, et al., Phys. Rev. Lett. 121, 132501 (2018).
65. Y.F. Niu, G. Colo, and E. Vigezzi, Phys. Rev. C 90, 054328(2014).
66. Y.F. Niu, G. Colo, E. Vigezzi, C.L. Bai, and H. Sagawa, Phys. Rev. C 94, 064328 (2016).
67. M. Sasano, H. Sakai, Y. Yako, et al., Phys. Rev. C 79, 024608 (2009).